

PIV and LDA Measurements of Secondary Flow in a Meandering Channel for Overbank Flow

Ishigaki, T.*¹, Shiono, K.*² and Rameshwaran, P.*³

- *1 Ujigawa Hydraulics Laboratory, DPRI, Kyoto University, 612-8235, Japan.
e-mail: ishigaki@uh31.dpri.kyoto-u.ac.jp.
- *2 Department of Civil and Building Engineering, Loughborough University, LE11 3TU, UK.
e-mail: K.Shiono@lboro.ac.uk.
- *3 Center of Ecology and Hydrology, Wallingford, OX10 8BB, UK.
e-mail: ponr@ceh.ac.uk.

Received 30 July 2001.
Revised 1 February 2002.

Abstract: Secondary flow in a compound meandering channel with straight floodplain banks for overbank was investigated by a visualization method and velocity measurement using three-component laser Doppler anemometer (LDA). The secondary flow in a cross section was visualized by the neutral buoyant tracer method with a submersible video camera. Secondary flow vectors in a cross section were obtained by using PIV software with captured frames from video source through PC and also by LDA measurements. From the comparison of the PIV and LDA results, it is found that PIV data show good agreement in quality with LDA measurements when the secondary flow is strong and stable as shown in this paper.

Keywords: visualization of secondary flow, PIV, LDA measurement, compound meandering channel.

1. Introduction

Severe flooding occurs worldwide every year as urban areas and agricultural lands are inundated. This threatens all kinds of natural life as well as damaging national economies due to the production loss and the cost of repairs. This kind of flooding is particularly severe on continental land masses but is also a frequent occurrence even for islands such as Japan and UK. In high river flow conditions, rivers often are running in an overbank condition and flooding adjacent plains, and a large exchange of momentum takes place between a faster flow in a main channel and a slower flow in a flood plain. There are also secondary flows generated by anisotropic turbulence arising from the irregularity of the boundary in a straight compound channel, and the flood plain flow rolling over the main channel flow in a meandering compound channel.

The flow in a compound meandering channel has following aspects (Willems and Hardwick, 1993; Ervine et al., 1993; Fukuoka et al., 1997; Shiono and Muto, 1998; Ishigaki et al., 1999 and 2000a; Ishigaki and Muto, 2000b).

- 1) Flow over flood plain is running straight when flooding depth is deep.
- 2) The structure of secondary flow is different from that in a simple meandering channel.
- 3) Fluid mixing between main channel and flood plain flow is stronger than that in a straight channel. The reasons why this is stronger are that fluid from flood plain and main channel are crossing each other and a secondary flow is produced there by the centrifugal force and the turbulent shear stress.
- 4) The secondary flow shows a spiral motion called secondary flow cell and affects the scouring and deposition of

channel bed. The cell makes sand bars (ridges) in the case that the main channel has a movable bed.

As the flow structure is complicated as mentioned above, the flow has not been fully investigated. In this paper, it is the objective to clarify the characteristics of the secondary flow on the basis of the results obtained by LDA measurements and the direct visualization method of the secondary flow in a cross section. And it is also the purpose to make a comparison of the LDA data and the PIV data.

2. Experimental Method

The test flume is 2.4 m wide 13 m long and 0.5 m deep with a sand re-circulation facility. A meandering channel was set in the form of a 120 degree meandering channel with a crossover length of 750 mm and a flat bed by placing polystyrene boards as flood plains whose surface is hydraulically smooth.

Three meanders were built in the flume. The sinuosity (= curved channel length/meandering wavelength) of channel is 1.38 and the valley slope is 0.002. The channel configuration and the bed form in the measuring section are shown in Fig. 1. Uniform sand with a mean diameter of 0.85 mm was used in the main channel. The main channel flow depth was initially set to 40 mm with the same slope as the valley had, which has given an aspect ratio b/h of 10. Velocity measurements were carried out using a TSI 3-component laser Doppler anemometer (LDA) after the bed was fixed by mortar. Measured locations are shown in Fig. 2.

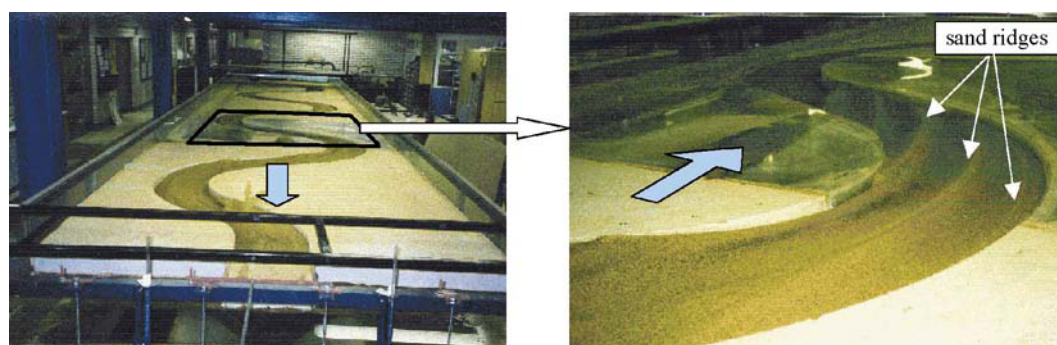


Fig. 1. Compound meandering channel and the bed form in the measuring section.

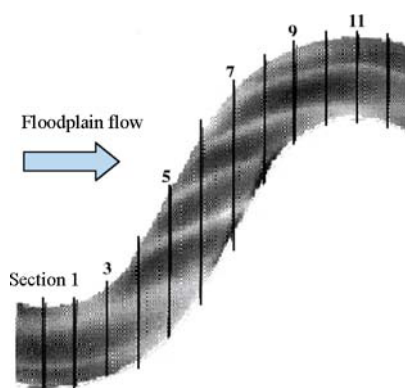


Fig. 2. Bed form and section number for LDA measurement.

The bed form was shown in Fig. 1 and Fig. 2, of which three-dimensional morphological bed form was measured using automated digital photogrammetry (Rameshwaran et al., 1999). It should be noted that the figure was plotted in gray scale. Deeper area is expressed by darker color and shallower area is expressed by light color. A number of distinct sand bars (ridges) crossing main channel with an angle start appearing near the upstream main channel bank.

An investigation of the secondary flow structure in the main channel was carried out using a submergible

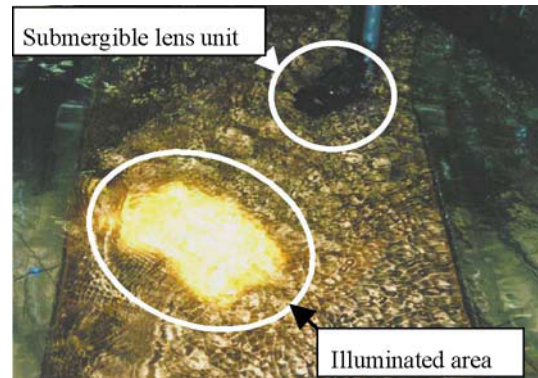


Fig. 3. Experimental set-up for visualization.

lens with a remote controlled video camera to visualize the secondary flow. Neutral-buoyancy plastic beads (a diameter of 0.45 mm with a specific gravity of 1.05) as tracers were released at about 1 m upstream of the test section with a minimum disturbance. The lens was set at about 300 mm downstream from the test section. The test section was illuminated with an ordinary slide projector with a power of 150 W (Fig. 3). A captured video source was processed by commercially available software (PhotoShop). More details for the visualization method can be seen in the literatures (Ishigaki et al., 1999 and 2000a; Ishigaki and Muto, 2000b). Secondary flow vectors in a cross section are obtained by using PIV software (VISIFLOW, AEA Technology) with captured frames from video source through a PC.

In this paper, all data are obtained in the case of $Dr = 0.45$. Dr is the relative depth that is the ratio of main channel and flood plain depth. The hydraulic conditions are as follows; the discharge Q is $0.0308 \text{ m}^3/\text{s}$, the flood plain depth hf is 3.28 cm, the mean velocity Um is 0.314 m/s, the hydraulic radius R is 3.72 cm, and Froude number $Fr = Um/(gR)^{1/2}$ and Reynolds number $Re = UmR/\nu$ are 0.52 and 11700 respectively.

3. Secondary Flow in a Cross Section

Secondary flows in some cross sections along a trough, where it was between two ridges as shown in Fig. 2, were visualized by the neutral buoyant tracer method as shown in Fig. 4. Spiral motions and separations behind the crest of sand ridges can be clearly observed. The spiral motions are called as a secondary flow cell induced by the shear stress between main channel and flood plain flows. The separating flow produces another secondary flow cell. Scales of both secondary flow cells are developing along a trough. Figure 5 shows the same separating flow behind a crest and secondary flow cells in the crossover section (Section 5). It is found that some part of fluid in a secondary flow cell flows over the crest, and then the fluid separates from the crest and produces a new secondary flow cell. The visualized motions can be also recognized in the distributions of secondary flow vectors obtained by LDA.

Several measurements of secondary flow vectors by LDA were also carried out along a trough and their results for $Dr = 0.45$ are shown in Fig. 6, together with the location of the measurement sections. It is clearly seen from Fig. 6 that the anti-clockwise secondary flow cell is generated at the edge of the floodplain, Section 6. This cell increases in size while the bed level gets deeper between Sections 6 and 9, meaning that the bed erosion occurs, then decreases in size as the bed level gets shallower after Section 8 and finally disappears. It is noticed that there is a clockwise secondary flow cell on the right side of the ridge generated by the cross-flow over the ridge (see Sections 7-9). This cross-flow is actually the anti-clockwise secondary flow generated by the flood plain flow between the next upstream ridge and this ridge. This cell increases in size and there is no cross-flow over the ridge at Section 10, however the strength of the cell is weakened as if it is a residual flow. The evidence of weakening the cell can be seen from reducing the bed level after Section 9 in the latter reach of the sand bar. Those two cells work each other as a counter flow to maintain a regular wavy bed form. It can be said that a number of secondary flow cells are initiated by interaction between the main channel flow and flood plain flow, as mentioned before. These cells increase the strength as flood depth increases and then make sand bars crossing the main channel at the flood depth.

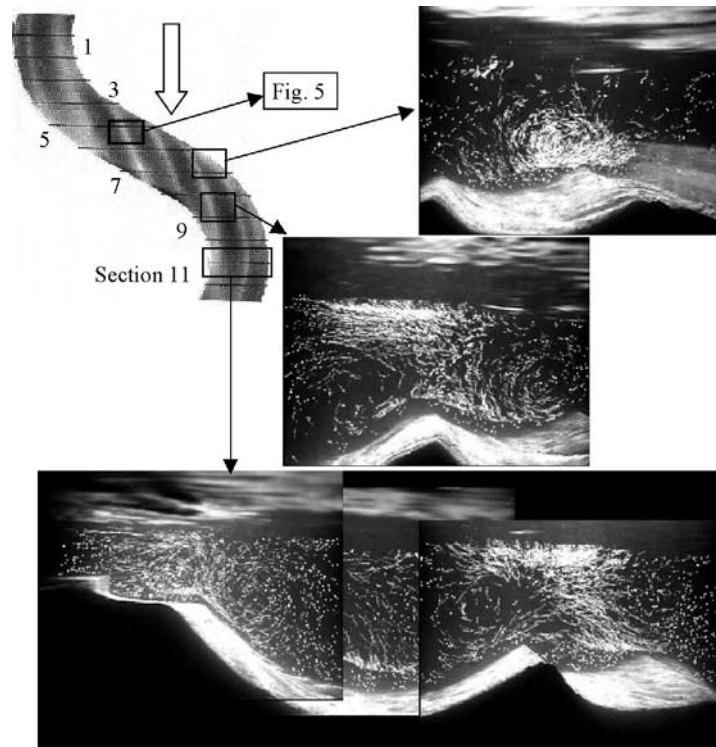


Fig. 4. Secondary flows visualized by neutral buoyant tracers in three cross-sections of flow.

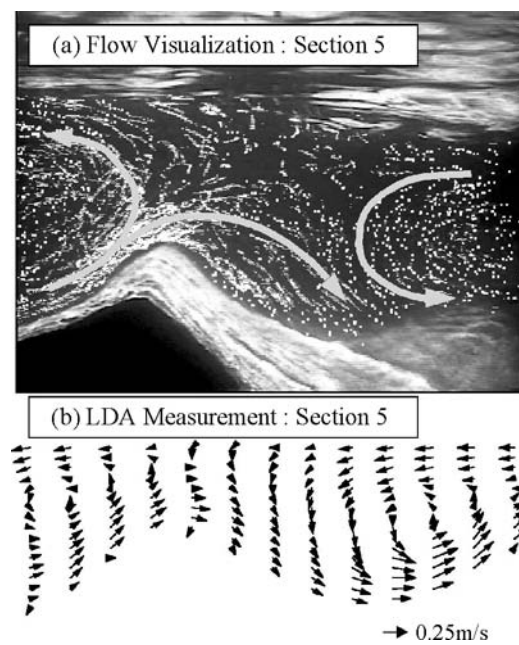


Fig. 5. Secondary flow cells and separating flow behind a crest in crossover.

To make a comparison between PIV and LDA data, both results at the bend apex (Section 11) for $Dr = 0.45$ are shown in Fig. 7. It can be seen from the figure that both PIV and LDA results match very well in quality. There are a number of secondary flow cells observed in this section, for instance, Cell A and B. Observable area of the cells is almost the same, but there are some differences in scale, magnitude and location of the center of the cell. The reason is that PIV data shows an instantaneous area of the cell and LDA data shows outline of the observable area of the cell.

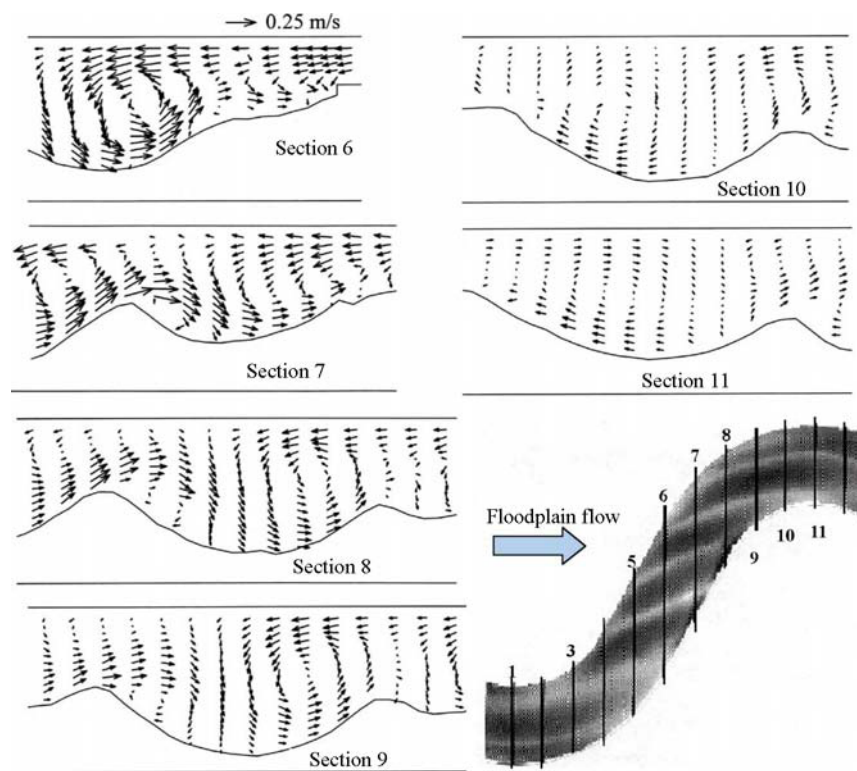


Fig. 6. Secondary flow vectors measured by LDA along a trough.

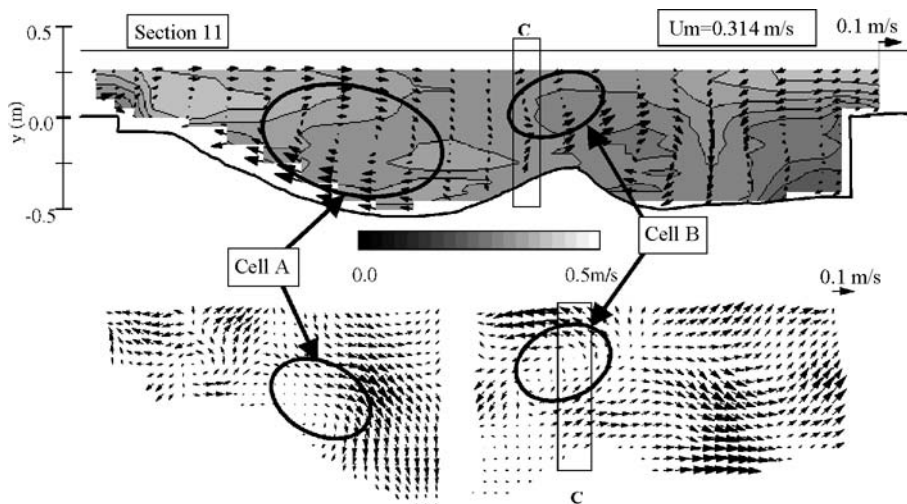


Fig. 7. Comparison of secondary flow vectors obtained by LDA (the upper figure) with those by PIV (the lower figure), together with the contour of longitudinal component of velocity, u , in Section 11.

The magnitude of velocity obtained by PIV was underestimated at about 40 percent as compared to LDA results. The discrepancy between both data mainly comes from the reading error of particle's position caused by the thickness of illuminated area. Thus, only a qualitative comparison of the LDA and PIV data was made here after PIV results were modified. The modification is that the mean value of the secondary flow by PIV is fitted for the value by LDA. This modification was made on the basis that the data obtained by LDA measurements were accurate. When a cell was stable and strong as the Cell B, the vertical distributions of magnitude by PIV and LDA show good agreement as shown in Fig. 8. In the other area, agreements in quality are not clear. Figure 9 shows the distribution of all PIV and LDA data in this section. From the results, it is found that the distributions of both data

are the same and that the magnitude distributes in the wide range. The mean value of magnitude normalized by the main flow velocity is large as compared to the value for a straight open channel flow, which is up to 0.1. It is also found that the value of the strongest secondary flow becomes up to 30 percent of the main flow velocity.

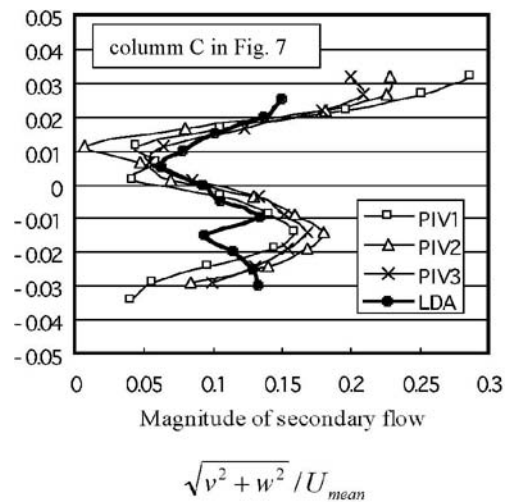


Fig. 8. Vertical distribution of secondary flow obtained by PIV and LDA.

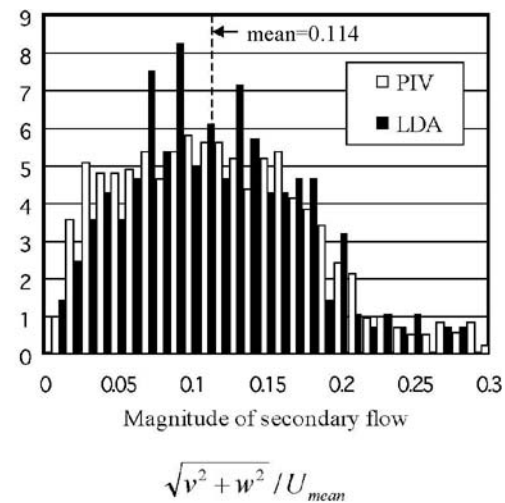


Fig. 9. Distribution of normalized magnitude of secondary flow obtained by PIV and LDA.

4. Conclusion

Three-dimensional structure of the flow in a meandering channel for overbank flow was discussed by using results obtained by a visualization method and velocity measurement. Secondary flow is the dominant fluid motion in this flow and visualized in a cross section of the flow by using a neutral buoyant tracer method with a submersible video camera. Main results are as follows.

- 1) Secondary flow cells were detected clearly by the flow visualization and LDA measurement.
- 2) Two types of secondary flow were observed in the experiments. One is induced by the shear stress between the main channel and the flood plain flows. The other can be observed at the downstream side of the crest of sand bar. The separation of the main channel flow behind the crest produces this secondary flow.
- 3) PIV data show good agreement in quality with LDA measurements when the secondary flow is strong and stable as shown in this paper.

References

- Ervine, D. A., Willets, B. B., Sellin, R. H. J. and Lorena, M., Factors Affecting on Conveyance in Meandering Compound Flows, *J. Hydr. Eng.*, 19-12 (1993), 1383-1399.
- Fukuoka, S., Ohgushi, H., Kanuma, D. and Hirano, S., Hydraulic Characteristics of the Flood Flow in a Compound Meandering Channel, *J. Hydraulics, Coastal and Environment Eng., JSCE*, No.579, II-41, (1997), 83-92 (in Japanese).
- Ishigaki, T., Muto, Y. and Sawai, K., Secondary Flow and Tractive Force in Compound Sinuous Channel, *Annual Journal of Hydraulic Engineering, JSCE*, 43 (1999), 329-334 (in Japanese).
- Ishigaki, T., Shiono, K., Rameshwaran, P., Scott, C. F. and Muto, Y., Impact of Secondary Flow on Bed Form and Sediment Transport in a Meandering Channel for Overbank Flow, *Annual Journal of Hydraulic Engineering, JSCE*, 44 (2000a), 849-854.
- Ishigaki, T. and Muto, Y., Flow Structure and Bed Form in Compound Sinuous Channel, *Proc. of 12th Congress of APD-IAHR, (Thailand)*, Vol.1, (2000b), 211-217.
- Rameshwaran, P., Spooner, J., Shiono, K. and Chandler, J. H., Flow Mechanisms in Two-Stage Meandering Channel with Mobile Bed, *Proc. of 28th Congress of IAHR Congress, (Graz, Austria)*, (1999), 259.
- Shiono, K. and Muto, Y., Complex Flow Mechanisms in Compound Meandering Channel for Overbank Flow, *Journal of Fluid Mechanics*, 376 (1998), 221-261.
- Willets, B. B. and Hardwick, R. I., Stage Dependency for Overbank Flow in Meandering Channel, *Int. Conference on River Flood Hydraulics*, (1993), 45-54.

Author Profile



Taisuke Ishigaki: He is Associate Professor in Ujigawa Hydraulics Laboratory, Disaster Prevention Research Institute (DPRI) of Kyoto University, Japan. He obtained his Doctor of Engineering from Kyoto University in 1994 and was a research associate of DPRI from 1981 to 1994. He was a guest researcher at University of Karlsruhe, Germany in 1987 and a visiting researcher of Loughborough University, UK in 2000. His research interests are Flood Disaster, River Hydraulics, Turbulence Structure of Open Channel Flow, Hydraulic Modelling, Flow Visualization and Flow Measurement.



Koji Shiono: He is Professor of Environmental Hydrodynamics, Loughborough University, UK. After a PhD in Civil Engineering, University of Birmingham, he worked as a research fellow at University of Birmingham from 1981 to 1989, a lecturer at University of Bradford from 1989 to 1993, and a senior lecturer at Loughborough University from 1994 to 1999. He has been a visiting lecturer at Kyoto University, a research fellow at Tokyo Institute of Technology and Kyushu Institute of Technology, a visiting professor at Kyushu University, Japan and a European Senior Fellow. His research interests are Hydrodynamics, Turbulence, Stratified Flow, River Hydraulics and Mathematical Modelling.



Ponnambalam Rameshwaran: He is a research scientist in the Centre for Ecology and Hydrology (CEH Wallingford). He obtained his PhD from the University of Aberdeen in 1998 and was a post-doctoral researcher in Department of Civil and Building Engineering, Loughborough University from 1998 to 2000. His research interests are Hydraulic/Mathematical Modelling, Sediment Transport, Turbulent Flow Structures, Computational Fluid Dynamics (CFD) and Flood Defence.